

12-14-2005

# Rescattering effects in the multiphoton regime

M. V. Frolov

*Voronezh State University, Voronezh, Russia*

A. V. Flegel

*Voronezh State University, Voronezh, Russia*

N. L. Manakov

*Voronezh State University, manakov@phys.vsu.ru*

Anthony F. Starace

*University of Nebraska-Lincoln, astarace1@unl.edu*

Follow this and additional works at: <http://digitalcommons.unl.edu/physicsstarace>



Part of the [Physics Commons](#)

---

Frolov, M. V.; Flegel, A. V.; Manakov, N. L.; and Starace, Anthony F., "Rescattering effects in the multiphoton regime" (2005). *Anthony F. Starace Publications*. 102.

<http://digitalcommons.unl.edu/physicsstarace/102>

This Article is brought to you for free and open access by the Research Papers in Physics and Astronomy at DigitalCommons@University of Nebraska - Lincoln. It has been accepted for inclusion in Anthony F. Starace Publications by an authorized administrator of DigitalCommons@University of Nebraska - Lincoln.

LETTER TO THE EDITOR

## Rescattering effects in the multiphoton regime

M. V. Frolov\*, A. V. Flegel\*, N. L. Manakov\*, and Anthony F. Starace†

\* *Department of Physics, Voronezh State University, Voronezh 394006, Russia*

† *Department of Physics and Astronomy, The University of Nebraska–Lincoln, Lincoln, NE 68588-0111, USA*

**Abstract.** The plateau features that characterize the low-frequency spectra of fundamental strong-field processes such as harmonic generation, above-threshold ionization and laser-assisted electron-atom scattering are shown to exist also for photon energies  $E_\gamma$  of the order of the energy  $|E_0|$  of a bound electron. The existence of these rescattering effects in such a high-frequency (and thus nontunnelling) regime is supported by accurate quantum analyses of intense Ti-Sapphire laser interactions with halogen negative ions, for which  $E_\gamma \approx 0.5|E_0|$ .

The rescattering scenario (RS) [1–3] is central to current understanding of fundamental strong-field processes such as above-threshold ionization/detachment (ATI/ATD), harmonic generation (HG) and multiple ionization owing to the insight it provides on the physics of strong laser-atom interactions, especially on the origin of plateau structures in high-energy ATI and HG spectra [4]. In the RS for these processes, the initial step is the laser ionization of a bound electron, which is assumed to escape by means of tunnelling, so that it has initially zero kinetic energy,  $E = 0$ . The next (main) step of the RS assumes that the electron may be returned by the driving laser field along a closed classical trajectory to the same (spatial) point where it was “born.” Quasiclassical analyses [4] show that the energies acquired by the electron from the laser field along its various trajectories have relative maxima,  $E_i$ , at return times  $\tau_i$  ( $\tau_0 < \tau_1 < \dots$ , where  $\tau_0$  is of the order of a laser period). The maximum energy gained is  $E_i^{\max} \equiv \mathcal{E}_{cl} \approx 3.1732U_p$ , where  $U_p = e^2F^2/(4m\omega^2)$  is the ponderomotive (or mean quiver) energy of a free electron in a laser field of amplitude  $F$  and frequency  $\omega$ . The energy  $\mathcal{E}_{cl}$ , a key quantity of the RS, is intimately related to the tunnelling step since it is the maximum energy that can be gained by a classical electron having zero initial energy; it corresponds to the trajectory having the shortest return time,  $\tau_0$ . In the final (re-collision) step of the RS, the laser-accelerated electron may (1) expend some of its accumulated energy  $E$  to excite a core electron (as in multiple ionization) or (2) recombine with the atomic core, converting its energy to harmonic photons (of maximum energy  $\hbar\Omega \approx |E_0| + \mathcal{E}_{cl}$ , where  $|E_0|$  is the ionization energy) or (3) scatter from the atomic core, thus contributing to one of the high-energy peaks on the ATI plateau, whose cut-off energy,  $E_{cut} \approx 10U_p$  [4], is also closely related to  $\mathcal{E}_{cl}$  (cf equations

(12)–(15) of [5]). Recently [5], the classical RS was used to interpret high-energy plateau structures in laser-assisted electron-atom scattering (LAES) spectra, based upon an accurate quantum analysis of LAES from a zero-range potential (ZRP) [6]. Moreover, although the plateau cut-off in LAES depends upon the incident electron energy  $E$ , for  $E \ll U_p$  it is approximately  $10U_p$ , as in ATI/ATD.

The RS, as well as the corresponding quasiclassical analyses of rescattering effects in strong-field processes, are relevant to an adiabatic (low-frequency) regime of laser-atom interactions,  $E_\gamma = \hbar\omega \ll |E_0|$ . In this regime, the concept of tunnelling is appropriate physically, and the use of stationary phase methods to perform the time integrations needed to evaluate transition amplitudes is justified mathematically. This regime is realized for femtosecond experiments with inert gases, in which, typically,  $E_\gamma \approx 0.1|E_0|$ . Quasiclassical simulations of rescattering effects and their interpretation in terms of interfering quantum orbits [4] are in good qualitative agreement with existing experiments and are supported by results of numerical integration of the time-dependent Schrödinger equation (TDSE) for both HG [7] and ATI [8].

In this letter, we analyse the evolution of plateau structures in the spectra of intense laser-atom processes as the photon energy increases from the tunnelling domain (characterized by  $E_\gamma \ll |E_0|$ ) to the “high-frequency” domain (characterized by  $E_\gamma \leq |E_0|$ ). Since for  $E_\gamma \approx |E_0|$  the tunnelling picture is not appropriate, we generally denote this nonperturbative regime of intense laser-atom interactions as the multiphoton regime. This latter regime is relevant to recent experiments on the interaction of standard femtosecond sources (i.e.,  $\lambda = 800$  nm) with negative ions [9] (in which case  $E_\gamma \approx 0.5|E_0|$ , where  $|E_0|$  is the electron affinity) and of intense infrared pulses (i.e.,  $\lambda = 3.5$   $\mu\text{m}$ ) with alkali atoms in excited states [10]; it also applies to forthcoming experiments for rare gases interacting with the intense vuv and soft x-ray radiation produced by free-electron lasers. Based upon an exactly solvable quantum model, we predict that plateau-like structures should appear in the spectra for all bound-bound (as in HG), bound-free (as in ATI/ATD) and free-free (as in LAES) multiphoton transitions in a high-frequency field having  $E_\gamma \leq |E_0|$  provided that the ponderomotive energy exceeds the photon energy, i.e.  $U_p \geq E_\gamma$ . These results thus provide a better understanding of the fundamental mechanisms for matter-light energy exchanges at photon energies comparable to the energy of a bound electron, when it may be expected that the quantum, multiphoton origin of the matter-light interaction becomes increasingly important.

The use of classical or quasiclassical models as well as the tunnelling concept is not justified at  $\hbar\omega \sim |E_0|$ ; thus, a proper theoretical analysis must be based upon a thoroughly quantum approach. To analyse the possible manifestations of rescattering effects in the multiphoton regime, we consider an electron in a short-range three-dimensional potential  $U(r)$  that vanishes outside a sphere of radius  $r_c$  and supports a single bound state,  $\psi_{\kappa lm}(\mathbf{r})$ , of energy  $E_0 = -\hbar^2\kappa^2/(2m)$  (where  $\kappa^{-1} \gg r_c$ ) and having s or p symmetry (i.e., angular momentum  $l$  equal to 0 or 1). We use the quasienergy state (QES) approach [11] to account nonperturbatively for electron interactions with both the potential  $U(r)$  and a strong monochromatic laser field,  $\mathbf{F}(t) = \hat{\epsilon}F \cos(\omega t)$ .<sup>1</sup>

Our treatment of the TDSE for a QES wavefunction is based on our recent time-dependent extension [13] of the effective range theory for low-energy electron scattering from a short-range potential [14], which we employed in [13, 15] to analyse initial state symmetry effects in ATD and which we extend here to analyze plateau

<sup>1</sup>Note that although very strong laser pulses are short, the concept of decay rates (and of the quasienergy formalism for their calculation) is applicable for pulse durations  $\geq 10$  fs [12].

features in both HG and LAES strong-field spectra. The key advantage of the effective range theory is that the results are largely insensitive to the shape of  $U(r)$ , since all information on  $U(r)$  is represented by only two parameters (see the parametrization of  $B_l$  in equation (4)). For bound-state problems, the parameters usually chosen are  $\kappa$  (or  $|E_0|$ ) and the coefficient  $C_{\kappa l}$  in the known asymptotic form of  $\psi_{\kappa lm}(\mathbf{r})$ ,

$$\psi_{\kappa lm}(\mathbf{r}) \approx C_{\kappa l} r^{-1} \exp(-\kappa r) Y_{lm}(\hat{r}) \quad \text{for } r \gg \kappa^{-1}. \quad (1)$$

For scattering problems these parameters are typically expressed in terms of the scattering length,  $a_p$  and the effective range,  $r_p$ . We regard here  $\kappa$  and  $C_{\kappa l}$  as the key (preassigned) parameters for characterizing a bound electron.<sup>2</sup>

The QES wavefunction in our approach has the standard Floquet form

$$\Psi_\epsilon(\mathbf{r}, t) = e^{-i\epsilon t/\hbar} \Phi_\epsilon(\mathbf{r}, t) = \sum_s \Phi_\epsilon^{s\omega}(\mathbf{r}) \exp(-(i/\hbar)(\epsilon + s\hbar\omega)t), \quad (2)$$

where the  $\mathbf{r}$ -dependence of the QES harmonics,  $\Phi_\epsilon^{s\omega}(\mathbf{r})$ , outside the potential  $U(r)$  (i.e.,  $r > r_c$ ) may be expressed analytically in terms of a time integral of the product of a periodic function,  $f_\epsilon(t) = \sum_s f_s \exp(-is\omega t)$ , and the Green's function for a free electron in a laser field  $\mathbf{F}(t)$  [13]. Numerically, then, the problem reduces to the determination of the function  $f_\epsilon(t)$  (or of the set of three such functions,  $f^{(m)}_\epsilon(t)$ , where  $m = 0, \pm 1$ , for the case of a bound state with p-symmetry). The function  $f_\epsilon(t)$  is the key object of our approach [13]. This function is sensitive to binding potential effects since it determines the behaviour of  $\Phi_\epsilon(\mathbf{r}, t)$  at small  $r$  ( $r \sim r_c$ )

$$\Phi_\epsilon(\mathbf{r}, t) \sim Y_{lm}(\hat{r}) \sum_s [r^{-l-1} + \dots + r^l B_l(\epsilon + s\hbar\omega)] f_s \exp(-is\omega t), \quad (3)$$

where the effective range parametrization is used for the coefficient  $B_l(\epsilon + s\hbar\omega)$ :

$$(2l-1)!!(2l+1)!! B_l(E) = -1/a_l + r_l k^2/2, \quad k^2 = 2mE/\hbar^2. \quad (4)$$

For *bound-state problems* (as in ATD and HG),  $f_\epsilon(t)$  satisfies a one-dimensional homogeneous (i.e., eigenvalue) integro-differential equation (cf [13]) for the complex quasienergy,  $\epsilon = \text{Re } \epsilon - i(\hbar/2)\Gamma$ , where  $\Gamma$  is the decay rate of an initial bound state  $\psi_{\kappa lm}$  (which evolves to the quasistationary QES (2) in a laser field). For *scattering problems* (as in LAES), the quasienergy  $\epsilon$  is real,  $\epsilon = E + U_p$  (where  $E = \mathbf{p}^2/(2m)$  is the electron energy), while  $f_\epsilon(t)$  satisfies an inhomogeneous integro-differential equation in which the inhomogeneous term equals the free-electron wavefunction (in the laser field) at  $r = 0$ . In both cases, the equations for  $f_\epsilon(t)$  may be represented as infinite systems of linear algebraic equations for the Fourier coefficients  $f_s$ , which permit an exact numerical solution over a wide interval of laser parameters.

Within the approach described above, we have performed analyses of the spectra of ATD, HG and LAES in the high-frequency domain,  $\hbar\omega \leq |E_0|$ . (For LAES, it is assumed that the potential  $U(r)$  describes the short-range potential of a neutral atom that supports a negative ion having a weakly bound, s- or p-state electron of energy  $E_0$ .) In all cases, exact expressions for the transition amplitudes may be presented in terms of generalized Bessel functions and Fourier coefficients  $f_s$  (cf [13, 15] for ATD; technical details of the HG and LAES calculations will be published elsewhere). As a basic example, we consider an  $F^-$  ion ( $|E_0| = 3.40$  eV) in a Ti-Sapphire laser field of  $\lambda = 800$  nm, in which case the ‘‘scaled’’ frequency is  $\tilde{\omega} = (\hbar\omega)/|E_0| = 0.456$ . To analyze

<sup>2</sup> Results for a ZRP model are a limiting case, i.e. for s-states,  $r_0 = 0$  (or  $C_{\kappa 0} = \sqrt{2\kappa}$ ) [15].

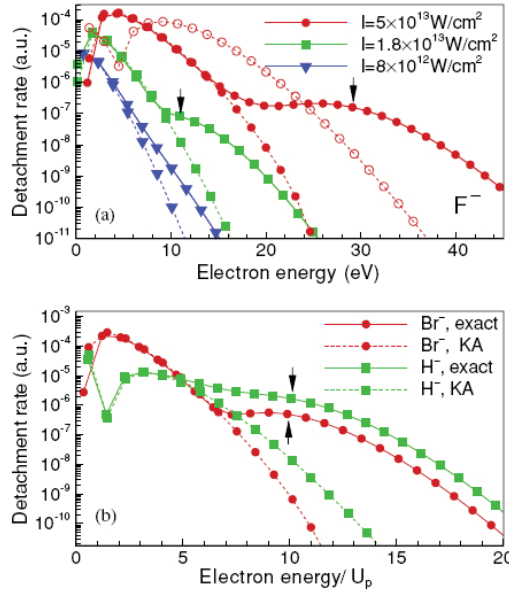


**Figure 1.** ATD spectra for (a)  $F^-$  for  $\lambda = 800$  nm  $\tilde{\omega} = 0.46$  and three intensities and (b)  $Br^-$  and  $H^-$  for equal scaled  $\tilde{\omega} = 0.46$  and  $I\tilde{p} = I/I_0 = 0.22$ . Solid lines: exact results; broken lines with solid symbols: length ( $L$ )-gauge KA results [17]; broken line with open circles: velocity ( $V$ )-gauge KA results for  $I = 5 \times 10^{13}$  W  $cm^{-2}$ . Arrows mark the  $10U_p$  cut-offs.

the species dependence of plateau features, we also present some results for other halogen ions for the same  $\lambda$ :  $I^-$  ( $|E_0| = 3.07$  eV,  $\tilde{\omega} = 0.505$ ) and  $Br^-$  ( $|E_0| = 3.37$  eV,  $\tilde{\omega} = 0.460$ ). To illustrate the bound-state symmetry dependence, results for  $H^-$  ( $|E_0| = 0.755$  eV) at  $\tilde{\omega} = 0.46$  ( $\lambda = 3.57$   $\mu m$ ) are also presented. It is also useful to introduce the “scaled” intensity,  $\tilde{I} = I/I_0$ , where  $I_0 = (mc|E_0|^3)/(4\pi e^2 \hbar^2)$ . (Note that  $I_0 \approx 1.37 \times 10^{14}$  W  $cm^{-2}$  for  $F^-$  and  $Br^-$  and  $1.50 \times 10^{12}$  W  $cm^{-2}$  for  $H^-$ .)

The evolution of ATD and HG spectra with increasing intensity is shown in figures 1(a) and 2(a) for  $F^-$  for three laser intensities, corresponding to the ratios:  $U_p/(\hbar\omega) \equiv \zeta = 0.31, 0.69$  and  $1.92$ . Species dependences are illustrated in figures 1(b) and 2(b). A key result is that multiphoton plateau features only appear for

$$U_p \geq \hbar\omega \quad \text{or} \quad \zeta \geq 1 \quad (5)$$

This result has a simple explanation since equation (5) is equivalent to the condition at which the perturbation theory expansion (in  $F$ ) for the complex quasienergy becomes divergent [16]. Thus, the high-frequency plateau features are inherent to the nonperturbative (and nontunnelling, i.e. multiphoton) regime of electron-laser interactions. For ATD, figure 1 also includes  $L$ -gauge Keldysh approximation (KA) results [17], to which our theory reduces if we neglect all coefficients  $f_s$  except  $f_0 = 1$  and take  $\epsilon = E_0 = -1$  [13, 15]. The exact and  $L$ -gauge KA results agree at low electron energies,<sup>3</sup> but disagree for high energies even at the lowest intensity shown in figure 1(a), for which there is no plateau feature. (Because the parameter  $\zeta$  is small in this latter case, the exact results indicate a perturbative ( $\sim \tilde{I}^n$ ) decrease of  $n$ -photon detachment rates with increasing  $n$ , without any signatures of rescattering.) Plateau structures in ATD, HG and LAES spectra are clearly visible in figures 1–3 in the nonperturbative regime,  $\zeta > 1$ . Surprisingly, the plateau cut-off positions for all these

<sup>3</sup>As argued in [13] and illustrated in figure 1(a), the  $V$ -gauge KA results fail to match the (gauge invariant) exact results at lower electron energies in the case of a p-state negative ion (see also [18]).

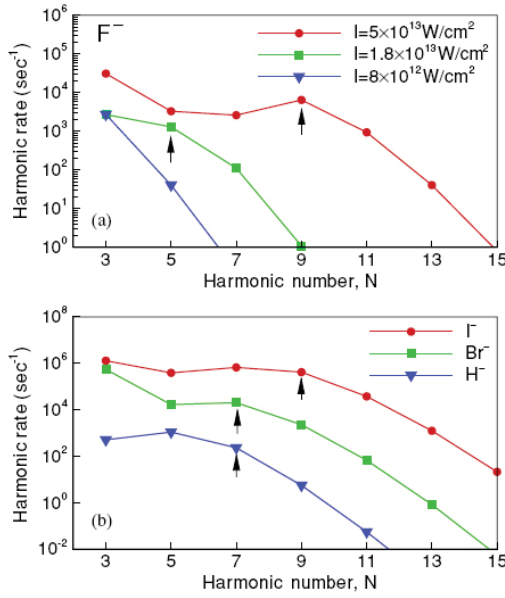


**Figure 2.** (a) HG spectra of F<sup>-</sup> for the same laser parameters as in figure 1(a). (b) HG spectra of Br<sup>-</sup> and H<sup>-</sup> (for the same laser parameters as in figure 1(b)) and of I<sup>-</sup> for λ = 800 nm and I = 5 × 10<sup>13</sup> W cm<sup>-2</sup> ( $\tilde{\omega} = 0.505$ ,  $IP = 0.49$ ). Arrows show the cut-offs,  $N_{\max} = (|Re \delta| + E_{cl})/(\hbar\omega)$ .

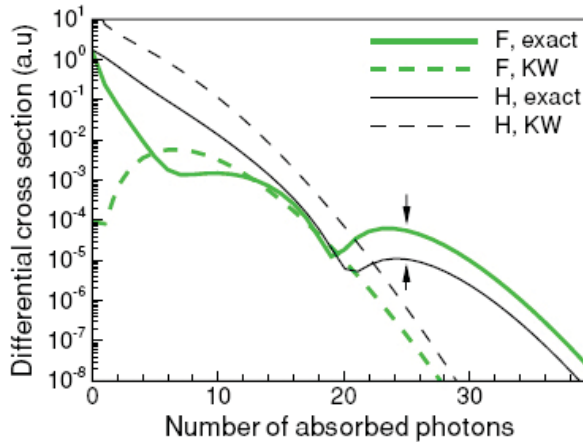


**Figure 3.** LAES cross sections for forward scattering (in the laser polarization direction,  $\delta$ ) for e<sup>-</sup>-F and e<sup>-</sup>-H with laser parameters  $\tilde{\omega} = 0.456$ ,  $IP = 0.64$  and incoming electron energies  $E = 2U_p$  (i.e.,  $E = 10.5$  eV for F and  $E = 2.32$  eV for H). Broken lines: Kroll-Watson (low-frequency) approximation [19]. Arrows mark the classical cut-off positions [6].

processes perfectly agree with rescattering-based quasiclassical (low-frequency) estimates involving  $\mathcal{E}_{cl}$ . This fact allows one to interpret the plateau features in terms of the RS even at high frequencies. Both the quantum origin of these high-frequency plateau features and the “magic” classical quantity,  $\mathcal{E}_{cl}$ , must therefore be “hidden” within the exact quantum equations for the QES wavefunctions. As shown below, it is within plateau-like structures in the spectrum of the QES-harmonics  $\Phi_e^{s0}(\mathbf{r})$  (considered as a function of  $s$ ) in the harmonic composition (2) of  $\Psi_e(\mathbf{r}, t)$  that we shall find the quantum origin of these key features of all strong-field processes.

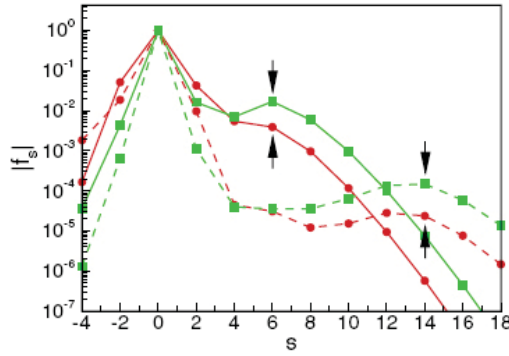


**Figure 4.** Plateau features in the spectra of Fourier coefficients  $f_s$  (normalized to  $|f_0| = 1$ ) for  $\text{Br}^-$  (circles) and  $\text{H}^-$  (squares) at the same  $\tilde{\omega}$  and  $IP$ . Solid lines:  $\tilde{\omega} = 0.46$ ,  $IP = 0.22$ ,  $\zeta = 1.15$ ; broken lines:  $\tilde{\omega} = 0.155$ ,  $IP = 1.44 \times 10^{-2}$ ,  $\zeta = 1.93$ . Arrows mark the cut-offs,  $s_{\text{max}} = (|\text{Re } \epsilon| + E_{\text{cl}})/(\hbar\omega)$ .

In the framework of the quasienergy approach [20], the QES-harmonics  $\Phi^{s\omega}_\epsilon(\mathbf{r})$  in equation (2) are formed (“populated”) within a few laser cycles (due to intense multiphoton exchanges between the atom and the field) and lead to the establishment of a “steady” quasienergy state of a quantum system in an oscillating field. In the perturbative regime,  $I \ll I_0$ , the population of the QES harmonics decreases rapidly with increasing  $|s|$  ( $\sim \tilde{I}^{|s|}$ ). In the nonperturbative regime, however, the dependence of  $|\Phi^{s\omega}_\epsilon(\mathbf{r})|^2$  on  $s$  exhibits a remarkable “rescattering” (plateau-like) structure for positive  $s$ , starting from  $s \sim |\text{Re } \epsilon|/(\hbar\omega)$  (i.e., when the harmonic energy,  $E_s \equiv \text{Re } \epsilon + s\hbar\omega$ , in equation (2) becomes positive). The plateaus are most developed at small  $r$ , where the binding potential effects are important and persist over a distance (along the laser polarization direction,  $\hat{\epsilon}$ ) comparable to the amplitude of free-electron oscillations (or the effective size of a closed electron trajectory),  $\alpha_0 = (eF)/(m\omega^2)$ . They extend in energy up to  $E_s \approx \mathcal{E}_{\text{cl}}$ , i.e. up to the maximum energy acquired by a free electron along a closed trajectory in a laser field. Plateaus in the spectra of the QES harmonics for quasistationary QESs of  $\text{Br}^-$  and  $\text{H}^-$  at small  $r$  ( $r \sim r_c$ ) are shown in figure 4. For small  $r$ , only even ( $s = 2k$ ) harmonics  $\Phi^{s\omega}_\epsilon(\mathbf{r})$  are nonzero and are proportional to  $f_s$  (cf (3)):  $\Phi^{s\omega}_\epsilon(\mathbf{r}) \sim f_s r^{-l-1}$ . Inclusion of harmonics  $\Phi^{s\omega}_\epsilon(\mathbf{r})$  with increasing  $s$  in transition amplitude calculations shows that the plateau structures shown in figures 1–3 originate from those in the spectra of the QES harmonics shown in figure 4. For the data in figures 1 and 2,  $\alpha_0$  lies between  $2.3\kappa^{-1}$  and  $6.0\kappa^{-1}$ . Thus, together with  $\xi$ , the ratio of  $\alpha_0$  to the “radius”  $\kappa^{-1}$  of a bound state,  $\eta = \alpha_0\kappa$ , is a second characteristic dimensionless parameter of the problem, which in the rescattering regime should be at least a few times larger than the unity.<sup>4</sup>

To elucidate how  $\mathcal{E}_{\text{cl}}$  may be extracted from our quantum results, we note that the exact quantum expressions for the transition amplitudes contain integrals (over  $t$  and

<sup>4</sup>Note that the well-known Keldysh parameter,  $\gamma = \sqrt{|E_0|/(2U_p)}$  (which may also be represented as  $\gamma = \eta/(4\xi)$ ) is relevant only to the low-frequency regime (see, e.g., [17]) and does not enter explicitly into our general equations for the case of a high-frequency field,  $\tilde{\omega} \sim 1$ . In our approach, the two key parameters,  $\zeta$  and  $\eta$ , reduce to the single parameter  $\gamma$  only after using stationary phase approximations, i.e. in the limit  $\tilde{\omega} \ll 1$ , in which case the tunnelling concept is appropriate. Nevertheless, for the data in figures 1(a) and 2(a),  $\gamma = 1.87, 1.26$  and  $0.76$ , for the three (increasing) intensities considered. Thus, even in the tunnelling picture, the data for  $\gamma = 1.26$  in figures 1(a) and 2(a) (where the plateau signatures are already clearly visible) correspond to the “low-frequency multiphoton” regime,  $\gamma > 1$ .

$\tau$ ) involving the functions  $\exp[(i/\hbar)S(t + \tau, t)]$ , where  $S(t + \tau, t) \equiv S(\mathbf{r} = 0, t + \tau; \mathbf{r}' = 0, t)$  is the classical action for a free electron in a laser field along a closed trajectory of period  $\tau$  that begins at time  $t$ . The energy gained,

$$\Delta E(t + \tau, t) = -\partial S(t + \tau, t) / \partial t, \quad (6)$$

has a global maximum at  $\omega\tau_0 = 4.086$  (and  $2\omega t = (\pi/2) - \omega\tau_0$ ), which is equal to  $\mathcal{E}_{cl} = 4U_p \sin^2(\omega\tau_0/2) \approx 3.1732U_p$ . In the perturbative regime, all “memory” of  $\mathcal{E}_{cl}$  is lost upon expanding  $\exp[(i/\hbar)S(t + \tau, t)]$  in  $F$ . In the nonperturbative, but low-frequency case, after using stationary phase methods,  $\mathcal{E}_{cl}$  explicitly enters the analytical results for the cut-off positions (cf [5]). In the general case, when the problem does not involve any small parameters,  $\mathcal{E}_{cl}$  nevertheless continues to reveal implicitly the classical properties of a quantum system in the strong laser field regime and these properties become more distinct with increasing laser intensity.

In conclusion, we have shown that the RS is applicable even in a high-frequency field, when multiphoton transitions (and not tunnelling) are its first step. In quantum language, high-energy plateaus originate from highly populated QES harmonics of the QES wavefunction (with energies up to  $\mathcal{E}_{cl}$ ) and this statement is equally valid in both low- and high-frequency fields. Our quantum analysis of plateau structures in strong-field processes is accurate for short-range potentials and our numerical results for the ATD spectrum of  $F^-$  support the interpretation of experiments [9] in terms of rescattering. Since our qualitative interpretations of plateau structures in terms of parameters such as  $\mathcal{E}_{cl}$ ,  $\xi$ , and  $\eta$  are general, we expect that our conclusions should be qualitatively valid also for ATI and HG processes in neutral atoms. Nevertheless, in a high-frequency field the Coulomb perturbation of free-electron trajectories may be more important than in the low-frequency case (because for  $\hbar\omega \approx |E_0|$  the inequality  $\alpha_0 \gg \kappa^{-1}$  (i.e.,  $\eta \gg 1$ ) cannot be realized for moderate laser intensities less than  $I_0$ ). Thus, the quantitative estimate of Coulomb effects in the high-frequency RS for long-range potentials by means of numerical integration of the TDSE is desirable.

## Acknowledgments

This work was supported in part by NSF grant PHY-0300665, by RFBR grant 04-02-16350 and by the joint grant VZ-010-0 of the CRDF and the RF Ministry of Education. AVF and MVF acknowledge the support of the “Dynasty” Foundation.

## References

- [1] Kuchiev M Yu 1987 *Zh. Eksp. Teor. Fiz. Pis. Red.* **45** 319; Kuchiev M Yu 1987 *JETP Lett.* **45** 404 (Engl. Transl.)
- [2] Schafer K J, Yang B, DiMauro L F and Kulander K C 1993 *Phys. Rev. Lett.* **70** 1599
- [3] Corkum P B 1993 *Phys. Rev. Lett.* **71** 1994
- [4] Becker W, Grasbon F, Kopold R, Milosevic D B, Paulus G G and Walther H 2002 *Adv. At. Mol. Opt. Phys.* **48** 35
- [5] Flegel A V, Frolov M V, Manakov N L and Starace A F 2005 *J. Phys. B: At. Mol. Opt. Phys.* **38** L27
- [6] Manakov N L, Starace A F, Flegel A V and Frolov M V 2002 *Zh. Eksp. Teor. Fiz. Pis. Red.* **76** 316; Manakov N L, Starace A F, Flegel A V and Frolov M V 2002 *JETP Lett.* **76** 256 (Engl. Transl.)



- [7] Krause J L, Schafer K J and Kulander K C 1992 *Phys. Rev. Lett.* **68** 3535
- [8] Bauer D 2005 *Phys. Rev. Lett.* **94** 113001
- [9] Pedregosa-Gutierrez J, Orr P A, Greenwood J B, Murphy A, Costello J T, Zrost K, Ergler T, Moshhammer R and Ullrich J 2004 *Phys. Rev. Lett.* **93** 223001
- [10] Paul P M, Clatterbuck T O, Lyngå C, Colosimo P, DiMauro L F, Agostini P and Kulander K C 2005 *Phys. Rev. Lett.* **94** 113906
- [11] Manakov N L, Ovsiannikov V D and Rapoport L P 1986 *Phys. Rep.* **141** 319
- [12] Day H C, Piraux B and Potvliege R M 2000 *Phys. Rev. A* **61** 031402 Becker A, Plaja L, Moreno P, Nurhuda M and Faisal F H M 2001 *Phys. Rev. A* **64** 023408
- [13] Frolov M V, Manakov N L, Pronin E A and Starace A F 2003 *Phys. Rev. Lett.* **91** 053003
- [14] Landau L D and Lifshitz E M 1992 *Quantum Mechanics* 4th edn (Oxford: Pergamon) section 133
- [15] Frolov M V, Manakov N L, Pronin E A and Starace A F 2003 *J. Phys. B: At. Mol. Opt. Phys.* **36** L419
- [16] Manakov N L and Fainshtein A G 1981 *Teor. Mat. Fiz.* **48** 375; Manakov N L and Fainshtein A G 1982 *Theor. Math. Phys.* **48** 815 (Engl. Transl.); Potvliege R M and Shakeshaft R 1990 *Phys. Rev. A* **41** 1609
- [17] Gribakin G F and Kuchiev M Yu 1997 *Phys. Rev. A* **55** 3760
- [18] Bauer D, Becker W and Milosevic D B 2005 *Phys. Rev. A* **72** 023415
- [19] Kroll N M and Watson K M 1973 *Phys. Rev. A* **8** 804
- [20] Zel'dovich Ya B 1973 *Usp. Fiz. Nauk* **110** 139; Zel'dovich Ya B 1973 *Sov. Phys. - Usp.* **16** 427 (Engl. Transl.)